Further study on iterative control loop for aberration correction in imaging systems with single mode fibre aperture

M. R. NASIRIAVANAKI[a], G. DOBRE[b], M.-A. PAUN[c*], A. HOJJATOLESLAMI[a], A. GH. PODOLEANU[b]
[a]*Research and Development Centre, School of Biosciences, University of Kent, Canterbury, CT2 7PD, United Kingdom*
[b]*Applied Optics Group, School of Physical Sciences, University of Kent, Canterbury, CT2 7NH, United Kingdom*
[c]*Electronics Lab, EPFL (Swiss Federal Institute of Technology), CH-1015 Lausanne, Switzerland*

An iterative control system was designed for compensation of wavefront aberration utilizing a micromachined deformable mirror through simulated annealing algorithm. 37 elements within a deformable mirror are controlled individually in a closed-loop to maximize the output optical intensity collected in a single mode aperture. In this paper, the design of the control system is explained comprehensively. The effect of the parameters involved on the achievable accuracy, computational load and speed of the algorithm are investigated. The shape of the mirror's surface throughout the runtime of the algorithm is also monitored and analyzed.

(Received March 20, 2013; accepted June 12, 2013)

Keywords: Optical fibre system optimization, Simulated annealing algorithm, Adaptive optics, Matlab, Mex file

1. Introduction

In an optical imaging system, collection of light backscattered from a sample is impaired by aberrations in the sample and the system, which result in a lower coupling efficiency of light into single mode fibre. Adaptive optics (AO) is a technology that can be used to compensate for the aberrations [1]. An AO system usually consists of a wave-front sensor (WFS) to measure the wave-front error, a deformable mirror (DM) and a control loop to apply the wave-front error inversely to the DM to compensate for the aberrations.

The need for a WFS raises the cost of the overall system, and there are also instances when they cannot be used, such as in microscopy [1, 2]. Moreover stray reflections from lens surfaces may affect the performance of the WFSs [2]. Open-loop beam-shape control can in principle be achieved without WFS using the knowledge of a DM's influence matrix.

However, the nonlinear characteristics of the DM make implementation of a wide range of pre-deformed shapes problematic. Hence, sensor-less methods for correcting distortions have been proposed [3-5]. In a sensor-less method, only a DM is required and a control closed-loop. The method operates iteratively to optimize a single measurable variable. The optimization operates on the mirror surface shape, towards reducing the wavefront error [6].

In a previous paper, we proposed an optimization technique that provides a simple, compact and affordable adaptive optic system to compensate for aberrations [7]. In this paper, we study the optimization algorithm in more details and investigate the reasons that alter its results. We add here an analysis of the shape of the DM while the program runs seeking optimization. We also aim to evaluate the accuracy and reproducibility of the technique in different situations and discuss the impact of certain parameters in producing better results and faster optimization.

2. Materials and Method

2.1 Optical system configuration

In the optical setup shown in Figure 1, light from a super luminescent diode (SLD) with the central wavelength of λ = 675.5 nm and $\Delta\lambda = 8.8\,\text{nm}$ is launched into a single mode optical fibre, OF1. The output light from OF1 is collimated by passing through a microscope objective (×10, N.A. = 0.25) and guided to lens $L_1$and lens L_2 to increase the beam diameter of approximately 3 times to cover the DM with a 15 mm diameter. The collimated beam of light is incident on the DM surface at an angle of 10º. The DM used is a micro machined membrane manufactured by OKO Technologies (Figure 1-inset) [8].

The membrane is very thin, circular in shape, and has a diameter of 15 mm. The membrane is mounted over a two-dimensional array of actuators placed in a hexagonal pattern. Any voltage difference applied between the membrane and each of 37 actuators results in the deformation of the membrane. The stroke range of the mirror is 6μm. The technology used in this mirror has made the mirror smaller and less expensive than piezoelectric transducer-based DMs which have also been used in blind optimization [9].

In the path from the DM, two lenses, L3 and L4 are used to reduce the diameter of the beam to allow its coupling into OF2 through a ×10 microscope objective. The OF2 terminates on an avalanche photodiode.

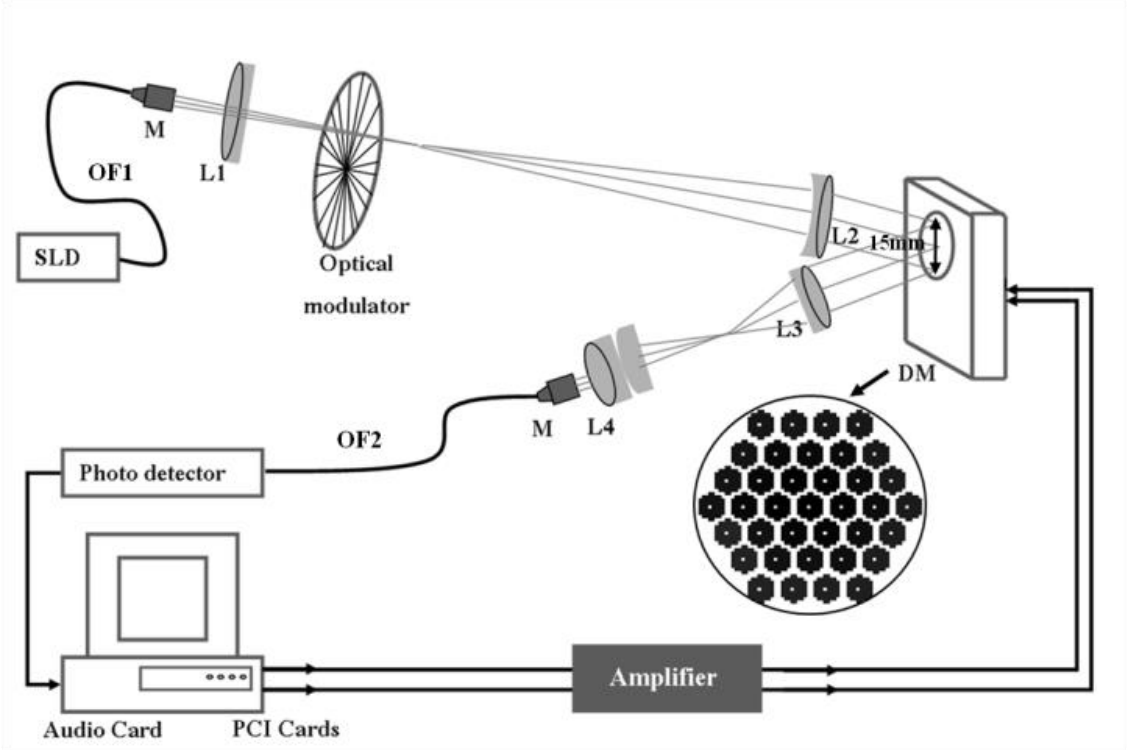

Fig. 1. Schematic of the optical system setup. (SLD: super luminescent laser diode, OF1-OF4: optical fibre, M: microscope objective, DM: 37-actuator deformable mirror, L1-L4: doublet lenses). Inset is an OKO micromachined deformable mirror. Location of the 37 actuators is shown.

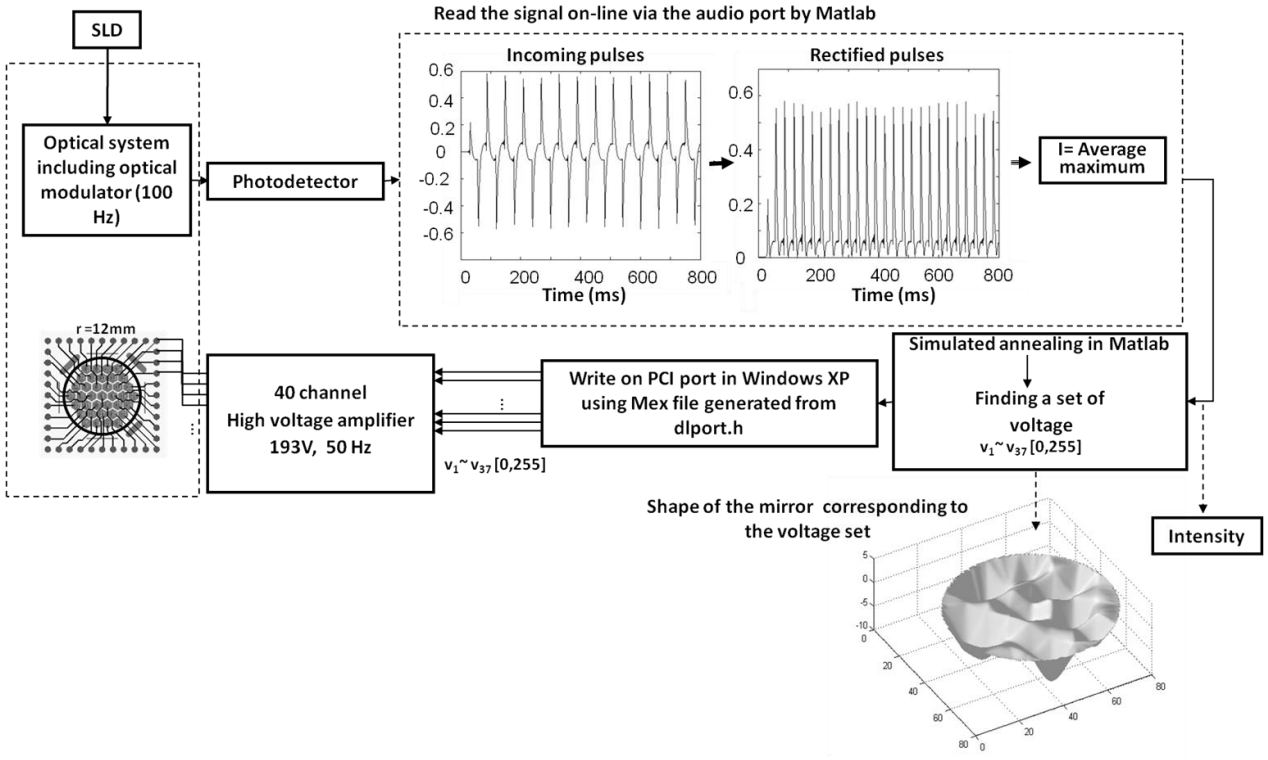

Fig. 2. Signal processing block diagram of the optimization setup. The dotted arrows show the final output after finishing the iterative algorithm

The electrical signal obtained from the photodetector is coupled into the input of the sound card (SC) (microphone port). The SC transfers the photodetector signal onto a personal computer (PC) in real time. As the SC is sensitive to ac signal only, a mechanical chopper was placed in the beam path. We operated the mechanical chopper at 100 Hz, sufficient for the signal to pass efficiently through the high pass filter in the sound card [8].

The optimization setup consists of a detector, SC, PCI card and the DM as shown in Figure 2. Signal from the SC is gathered using MATLAB for data acquisition. The signal is rectified and the amplitude of 10 incoming pulses is averaged to provide the control signal. The outliers of the peaks have been taken out before applying the averaging operation. This prevents acquiring the noisy signal due to the electronics noise. The output of the algorithm is a set of 37 values which are sent to the DM. The values are in the range between 0 and 255. We employ two 24-channel 8-bit PCI digital to analogue convertor (DAC) cards to write 8-bit values to the base address of each card which results in the corresponding analogue values on the channels of the PCI card's outputs.

We developed both the signal acquisition and processing in a single programming environment. We converted the port controller code written in Visual C++ to MATLAB using mex-files. Mex-files are a way to call custom Visual C++ routines directly from MATLAB as if they were MATLAB built-in functions [11]. The analogue voltages generated at the output of the PCI cards are amplified linearly to the range of 0 to 193V. The voltages are then applied to the mirror's 37 actuators simultaneously, and their values determine a certain shape for the membrane surface.

2.2 Optimization Algorithm

Simulated annealing (SA) introduced in 1982 by Kirkpatrick et al. [11], is a technique for combinatorial optimization problems, such as minimizing multivariate functions [12-13] to improve the so-called Travelling Salesman Problem [14]. SA is of interest here due to its efficiency and less computational complexity than all other known techniques that require an exponentially increasing number of steps as the problem becomes larger [12].

In comparison with iterative improvement methods, which can be simply trapped in local minima, SA improves the result by occasionally considering the worse situation [15]. SA is however a heuristic optimization technique which does not guarantee to output the optimum value [12].

The SA concept comes from a physical process of heating to a temperature that permits many atomic rearrangements, and then slowly cooling a substance allowing it to come to thermal equilibrium at each temperature until the material freezes into a shape that corresponds to a strong crystalline structure and/or the lowest crystal energy [15].

In a search problem looking for a global minimum, there will be different moves depending on the optimization algorithm. Unlike the iterative improvement method [11] which does not allow movement towards higher energy states, SA allows an occasional increase in energy caused by introducing some random perturbation, such as moving a particle to a new location. The resulting change in energy ΔE can be either negative (ΔE < 0), i.e. the new configuration has lower energy and is accepted as the starting point for the next move, or positive (ΔE > 0).

In the latter case the move may still happen [15]. In physical systems, jumps to higher energy states do happen, but they are moderated by the current synthetic temperature *T*. The probability of large uphill movements in energy is large at high temperatures, while at low temperatures is small. This process has been modeled by a Boltzmann distribution [11].

The probability of an uphill movement of size ΔE at temperature *T* is P which in the SA method is compared with a uniform random number R in the range [0,1]. Only if R<P, the uphill movement is accepted. Initially, this effective synthetic temperature is high enough to permit an aggressive random search of the configuration space i.e. most uphill movements are allowed.

As the synthetic temperature goes down, fewer uphill movements are allowed. At the coldest temperatures, very few disruptive uphill movements are permitted by the Boltzmann condition. In the low temperature regime, annealing closely resembles standard downhill-only iterative improvement [15]. In the context of adaptive optical control, the simulated annealing algorithm is well suited to the task because of its ability to independently optimize many variables at once [16].

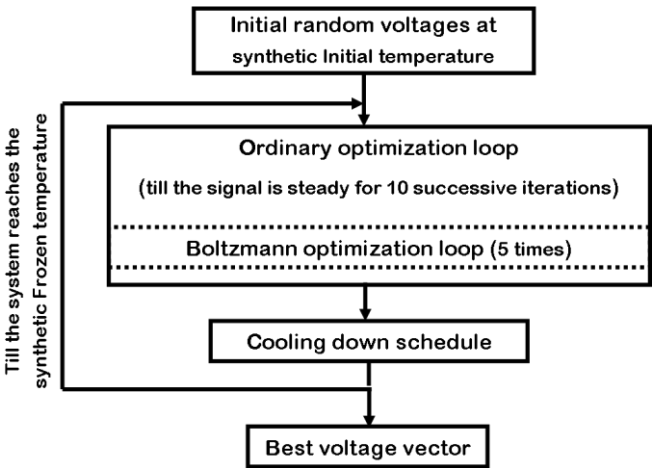

Fig. 3. Flowchart diagram of the simulated annealing algorithm applied to the deformable mirror for wavefront aberration correction

In simulated annealing there is a need of an optimization parameter or the common cost function in the optimization algorithms. In this study, the cost function is defined as the difference between the new intensity and the highest intensity detected up to that point, which we call Current Maximum Intensity (CMI). The variables are

the 37 components of a vector sent to the actuators. The vector controls the actuator voltages. The flowchart of the SA-based algorithm designed to find the best shape of the mirror's surface is given in Fig. 3.

In keeping with the terminology of SA, the artificial parameter, synthetic temperature, determines how often the algorithm switches between a local and a global search. The input values to the algorithm are a set of 37 variables which are chosen from the variable space. The variable space has values between 0 and 255 for each of the 37 variables which results in 37^{256} different sets. Finding a set which can correct the aberrations is the mission of the optimization algorithm.

The initial value of the synthetic temperature has to be high enough to let the algorithm choose any value in the whole variable space. The initial temperature (melt temperature) was experimentally considered to be 1000 and the final (frozen) temperature to be 0.001. The selection of these values is discussed further in the Results and Discussion section.

The algorithm begins with sending a random set of 37 between 0 and 255 through the PCI cards and the amplifier to the actuators. A uniformly distributed pseudo-random function with Gaussian distribution is chosen to generate the random values [16]. The maximum intensity is set to zero at the beginning. From now on, the algorithm operates in its *ordinary optimization loop* (OOL) while the synthetic temperature is examined to see whether or not it is still less than the frozen temperature. OOL is the local search procedure. The shape of the mirror is changed according to the actuator voltages and this produces a new value of photodetector current.

If the intensity is greater than the CMI value, it becomes the new CMI and also the voltage vector is saved as the best vector. At each synthetic temperature, the OOL is continued until a situation is reached where along 10 successive iterations, the rate of intensity increase becomes less than a threshold value.

An allowed variation of the intensity at each temperature was defined for the threshold value, which is constant for a determined range of the synthetic temperature; this is one temperature step. The threshold values are decreased by 10% for each temperature step decrease. Accordingly the allowed variation is progressively decreased.

As a result, the thermal equilibrium condition of the algorithm is obtained in a smaller range of intensity variation. Without the modification that we used on decreasing the synthetic temperature scheme, the convergence time of the algorithm will be longer. The cooling schedule is based on $T_{new}=0.9T_{old}$; in this study, the number of cooling-down steps based on our choice of initial and final temperatures is 132 steps. The best voltage set is the set which produces the CMI, best voltage is updated at each iteration.

In the OOL, at each iteration, the value of actuator voltages is updated in a random manner around the best voltage by adding/reducing one unit to/from the voltages individually. In the OOL, there is another loop, *Boltzmann optimization loop* (BOL) in which the value generated by the Boltzmann function is compared with a random value in the interval 0 and 1 (Boltzmann condition). If the value is greater than the random value, the algorithm is allowed to choose a random set in the whole variable space for 5 times (this value was optimized experimentally).

The variable space is however narrowed down iteration to iteration. If the intensity at this stage is higher than the CMI, it becomes the new CMI and the corresponding voltage set is recorded and becomes the best voltage set.

After reaching the thermal equilibrium at each temperature step, the synthetic temperature step is decreased. The process terminates when the synthetic temperature becomes lower than the frozen temperature. In the end, the optimal shape of the mirror's surface is determined by the "best voltage set" obtained from the algorithm, which leads to producing a higher intensity than when the optimization is not added to the system.

3. Results and discussion

The algorithm was tested on a 2GHz Pentium IV computer with a 1GB RAM. Different annealing schedules have been investigated. These schedules consist of three elements: initial temperatures T, final temperatures T_f and cooling schedule and the efficiency and convergence time (the speed) of the algorithm were evaluated.

We tested initial temperatures T = 10, 100, 400, 1000, 10000, final temperatures T_f =0.1, 0.001, and 0.0001, 0.00001, and investigated different cooling schedules $T_i=cT$, $T_i=T\cdot\exp(-i)$, $T_i=T\cdot\exp(-i/10)$, $T_i=T\cdot\exp(-i/1)$, where i is the index of iteration in the main loop and c is a multiplier that can take any value between 0.1 and 0.9.

To this aim, considering an appropriate runtime in order to achieve a higher number of maximum intensities, the initial and final temperatures obtained to be 1000 and 0.001, respectively.

Running several experiments with different schedules, was found that increasing the value of the initial temperature does not enhance the CMI but only extends the runtime. Choosing a smaller frozen temperature leads to achieving a better maximum intensity, although the changes after a certain temperature are tiny and the question arises of whether it is worth taking a longer time to reach a slightly better intensity. This will be discussed further later on.

Cooling schedule is chosen according to the generative function used in the simulated annealing algorithm; generative function is a distribution used to approximate the search space.

This distribution can be Normal, Boltzmann or Cauchy, depending on the variant of the simulated annealing technique used. The selection of the generative function, hence cooling schedule is based on the number of iterations and the nature of the problem, whether the dynamic range of the variables is large or small. Here the generative function is Boltzmann distribution function and the best schedule suited to this generative function is $T=T*0.9$. This was proved experimentally and reported in [17].

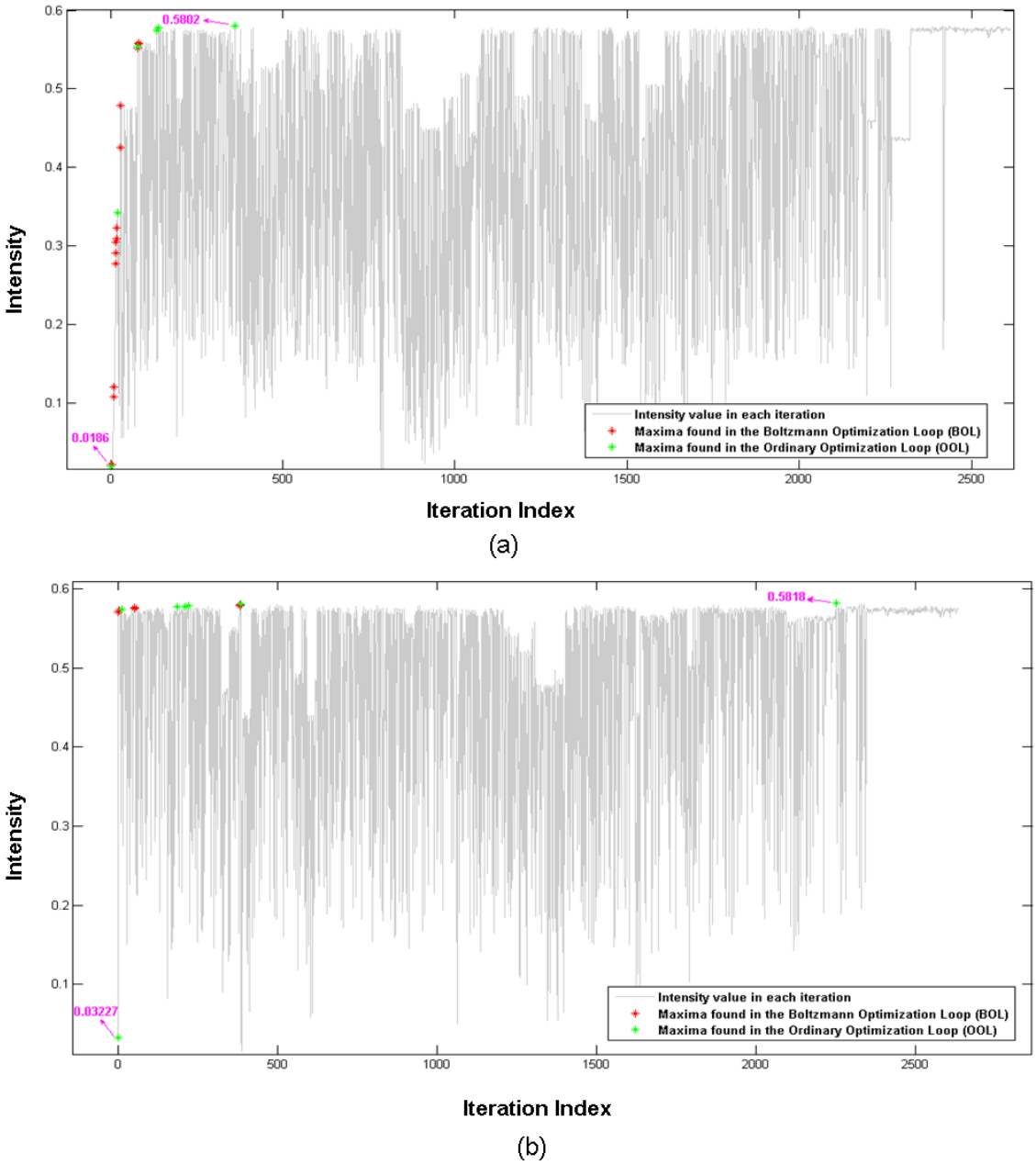

Fig. 4. (a and b) Intensity profiles monitored during 2600 iterations of the SA algorithm. The minimum and maximum achieved intensities are specified on the graph with pink arrows. In both images, the green asterisks show the improved intensity peaks obtained from the ordinary optimization loop (OOL) and the red asterisks show the improved intensity peaks obtained from the Boltzmann optimization loop (BOL).

The SA algorithm with the initial and final temperatures and the cooling schedule as described above was run. The progress of intensity while running the algorithm is given in Figure 4 (a and b).

As shown in Figure (4a), the photodetector current increased from 0.0186 mA to 0.5802 mA which demonstrates a 31-fold increase whereas in Figure (4b), the output intensity increased from 0.03227 mA to 0.5818 mA, corresponding to an 18-fold increase. However, we cannot claim that the algorithm is able to enhance the CMI by the order of around 31 or 18 times.

The only thing which could be said is that for an optical system with static aberrations, the proposed algorithm is able to find an appropriate shape of the mirror to compensate the aberration so that the system achieves the highest possible photodetector current. A part of improvement ratio depends on the start point of the algorithm. This will be explained further later on.

Looking at the progression of the intensity in Figure (4a), it can be noticed that in the first stages, the algorithm is fast such that in the first 82 iterations, the intensity in 16 steps has improved 30 times whereas during the next 57 iterations, there was no improvement, apart from two steps

which determined a 1.12 times improvement. The rest of the iterations did not improve the intensity any further.

In Figure (4b), the same graph as that in Figure (4a) is shown with a different intensity improvement profile. In this graph, there is a new maximum intensity at iteration number 2252 which shows that the algorithm is still active.

As seen in Figure 4 (a and b), the application of the Boltzmann condition resulted in large variations of the intensity. In the BOL, the algorithm looks for a set of 37 voltage values throughout the variable space that produces a higher intensity than CMI. The voltage values of the set are randomly changed in the interval between 0 and 255. The number of improved intensity peaks indicated by red asterisks in the graphs in Fig. 4 shows the significance of the use of the Boltzmann probability scheme.

As the algorithm reaches towards a lower synthetic temperature, the Boltzmann condition is fulfilled less likely and the OOL operates without going through the BOL. We examined our algorithm for a similar set-up to the one shown in Figure 1 on 14 different runs. Successively running the algorithm showed that, the maximum intensity value (with two significant figures) is obtained on average in 64 % of runs and the remaining 36% of runs give values with 95% of the maximum intensity (see Figure 5).

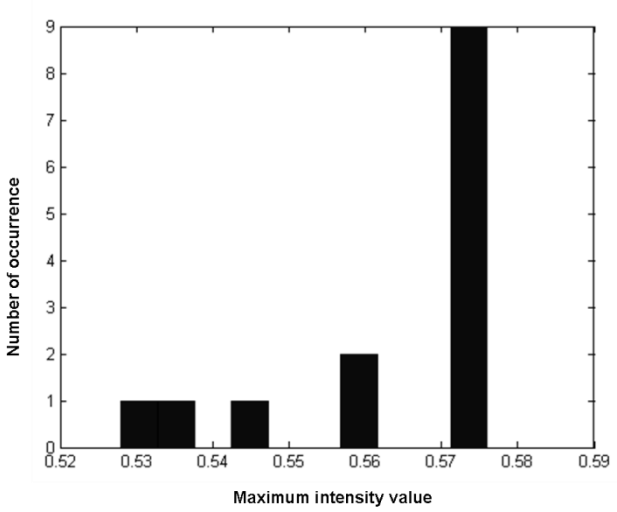

Fig. 5. Histogram of the maximum intensity values obtained from 14 runs for the optimization of the same system showing that 64% of runs result in maximum achievable intensity (i.e. above 0.57).

The number of iteration which produces the highest achievable intensity, varies from run to run; for instance it is achieved at iteration numbers 361 and 2252 in the experiment shown earlier in Fig. 4(a) and (b), respectively. The maximum was also achieved in fewer iterations (as few as 10) during other runs. In this respect, finding the optimal number of iterations using the principle of SA technique is still being investigated.

From the experiments we realized that in the standard form of the SA algorithm (with Boltzmann generative function), a shorter run time leads to a smaller maximum intensity, however a longer run time does not necessarily result in a larger maximum intensity. This statement is proven by the graph in Figure 6 which shows the maximum intensity obtained for different runtimes. In Figure 6, the initial achieved intensity, is the intensity obtained from the optical setup when voltage zero was sent to the actuators of the deformable mirror. For instance the experiments 6 and 7, have almost the same maximum intensity but their run time are over three minutes different, or in experiments 3 and 9 with the same run time, different maximum intensities are achieved.

The deformation produced by each actuator in membrane mirrors obeys the formula given in Equation 1.

$$\delta z(x,y) = -\frac{P(x,y)}{T} = -\varepsilon_0 \frac{V^2}{Td^2} \tag{1}$$

where δz is the deformation, ε_0 the vacuum permittivity, T is the membrane tension and P is the electrostatic pressure due to the voltage V across the gap between the membrane and the electrode, d , with the boundary condition $z = 0$ at the clamped edge of the membrane [18].

As shown in Figure 1, the mirror is hexagonal and the actuators are also arranged in a hexagonal fashion. We simulated the surface of the deformable mirror simplistically for 20 sets of voltages by using the voltage values sent to the actuators and an interpolation technique. For visualization, an azimuth angle of 60^o and elevation angle of 60^o are used. The mirror's surface and shape are shown in Fig. 7. This simulation was performed using the voltage sets obtained from the annealing schedule whose results have been given in Fig. (4a).

As seen, the mirror's surface shape is changed significantly during the optimization process. However, towards the end of optimization when the system reaches the final temperature, it changes only slightly from iteration to iteration. One of the challenging issues in SA is when to stop the algorithm. By measuring variation rate of the shape of the mirror's surface which is determined by the voltage values sent to the actuators, from an iteration to the next, and taking into account the updated CMI recorded at each iteration, one can set a stop constrain.

Compared to an adaptive optics system equipped with a WFS, the sensor-less approach however improves the optical system it has some downsides. In terms of speed, the aberration correction technique using the WFS takes sub seconds, whereas the sensor-less method using SA may require 20 minute to 2 hours for optimization. Another problem with SA, based on the observation we carried during several experiments, is that the defocus aberration can less likely be reduced.

This issue was revealed when in the imaging system used in [19, 20], we compared the aberration corrected images obtained from the WFS and those from the optimization technique. Not removing defocus aberration reduces the signal to noise ratio of the resultant image.

We did not obtain the best possible shape of the mirror's surface in the allocated time in every experiment we carried out (see the graph in Fig. 8). However when the

initial set of voltage values was chosen after running a random search algorithm, we did not observe this problem anymore. The random search algorithm generates sets of 37 values as the start set which makes the convergence time of the SA shorter. The algorithm used for the random search follows the parameters defined in BOL.

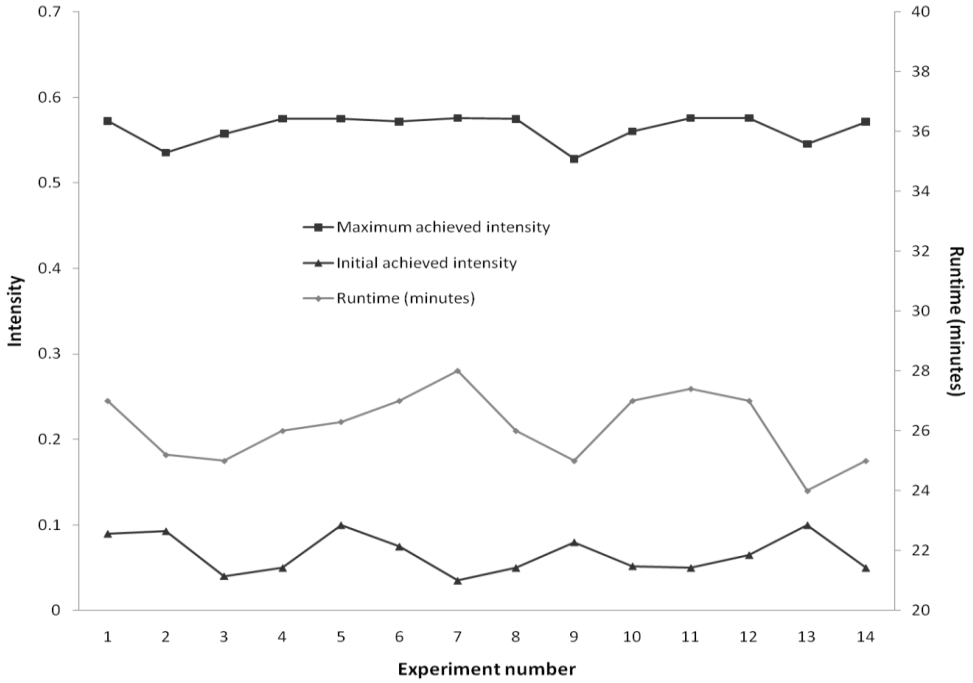

Fig. 6. Maximum achieved intensities and corresponding runtime for 14 runs of the algorithm to correct aberration of the same setup. The initial achieved intensity indicated in the graph is the intensity obtained from the optical setup when voltage zero was sent to the actuators of the deformable mirror.

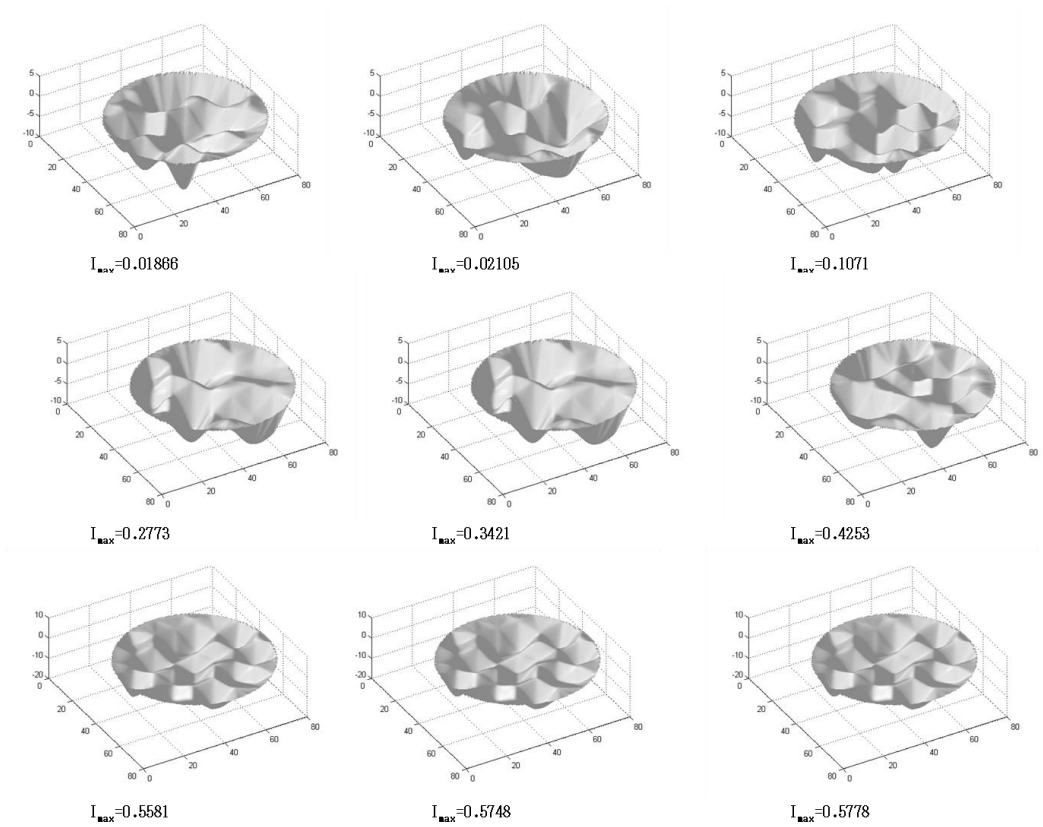

Fig. 7. Deformable mirror's surface shape at azimuth angle of 60^o with a 60^o elevation. The stroke range of the mirror is 6μm.

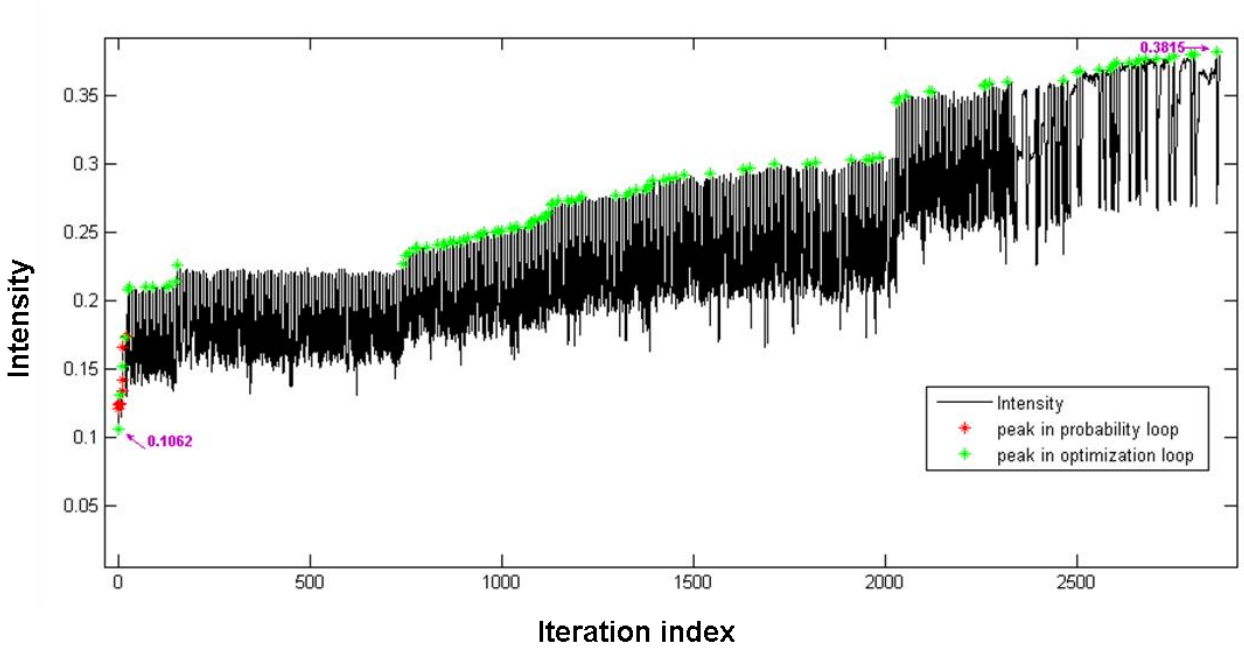

Fig. 8. Intensity profiles monitored during the SA algorithm in allocated time (30 minutes). The minimum and maximum intensities are specified on the graph with pink arrows. The green asterisks show the improved peak intensity obtained from the OOL and the red asterisks show the improved peak intensity obtained from the BOL.

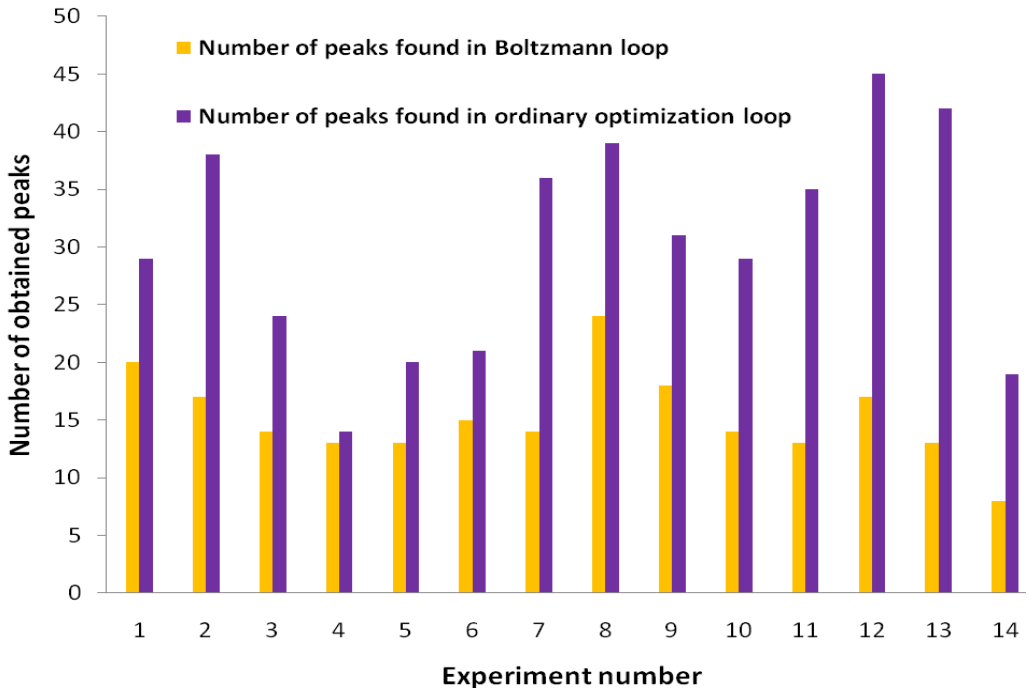

F*ig. 9. Bar graph of the number of peaks obtained by Boltzmann (pink) and ordinary (green) optimization loops during the SA algorithm.*

The number of iterations in the BOL is five times larger than the number of iterations in the OOL, however the number of maxima obtained by OOL is higher than those obtained by the BOL (Fig. 9).

We reduced the size of the variable space in BOL as the CMI improves using an intelligent search method. It eliminated the part of the variable space that has been already searched for the next iteration search, providing that it did not improve the CMI. This technique resulted in a higher number of maxima in a shorter time.

Another issue which affects the efficiency and convergence time of the SA algorithm is the dynamic range of the variables to be optimized. If the variables do not have a large dynamic range (variation of the value of

the variables is less than 10% of the maximum value), the algorithm can find the set of voltage value that produces the global maximum intensity rather easily [11]. However, when the algorithm searches many local peaks and the synthetic temperature is low, it takes long to climb down, thus trapping the solution to a local maximum [11]. We did not experience such a situation, possibly because the dynamic range of the voltage values was sufficiently low.

5. Conclusion

We have presented a simulated annealing (SA) algorithm for optimization of optical systems and showed that this algorithm is quite promising in finding a shape of the mirror's surface which produces the global maximum intensity, if the annealing schedule is chosen appropriately.

We used SA with sensor-less adaptive optics for aberration correction of an optical fiber system and demonstrated that optimization of an optical setup using SA is reproducible. The shape of the mirror' surface throughout the runtime of the algorithm is also monitored and analyzed.

By measuring variation rate of the shape of the mirror's surface which is determined by the voltage values sent to the actuators, from an iteration to the next, and taking into account the updated CMI recorded at each iteration, we set a stop constrain to terminate the SA algorithm.

We discussed the parameters that play important role in making the method faster and more accurate; initial temperature, final temperature, cooling schedule and number of iterations in the ordinary and Boltzmann optimization loops. We also mentioned the limitation of the algorithm in terms of timing and that it is application-oriented.

References

[1] M. L. Plett, P. R. Barbier, D. W. Rush, Appl. Opt. **40**, 327 (2001).
[2] D. Merino, C. Dainty, A. Bradu, et al., Optics Express, **14,** 3345 (2006).
[3] M. Booth, Optics Express, **14,** 1339 (2006).
[4] E. Grisan, F. Frassetto, V.Da Deppo, et al., Appl. Opt., **46,** 6434 (2007).
[5] C. D. Toledo-Suárez, M. Valenzuela-Rendón, H. Terashima-Marín, et al., On the Relativity in the Assessment of Blind Optimization Algorithms and the Problem-Algorithm Coevolution, p. 1436 (2007).
[6] L. Sherman, J. Ye, O. Albert, et al., J. Microsc. **206,** 65 (2002).
[7] M. A. Paun, M.R.N. Avanaki, G. Dobre, A. Hojjat, A.G., Podoleanu, J. Optoelectron. Adv. Mater. **11,** 1681 (2009).
[8] O. Soloviev, M. Loktev, G. Vdovin, *"Adaptive Optics Product Guide"*, April 2009 edn. (OKO technology, 2009), At: http://www.okotech.com, last accessed April, (2009).
[9] P., Yang, Y., Liu, W.Yang, et al., Opt. Commun., **278,** 377 (2007).
[10] M. MathWorks, *"The Language of Technical Computing"*, At: http://www.mathworks.com, last accessed April, (2009)
[11] Kirkpatric, S., Gelatt, C., Vecchi, M., *"Optimization by Simulated Annealing",* Science, **220,** 671 (1983).
[12] R. Rutenbar, IEEE Circuits Devices Mag., **5,** 19 (1989).
[13] R. Carr, Simulated Annealing, From *Mathworld* -A Wolfram Web Resource, created by Eric W. Weisstein, http://mathworld.wolfram.com/SimulatedAnnealing.html
[14] E. L. Lawler, A. Rinnooy-Kan, J. K. Lenstra, et al., "The traveling salesman problem: A guided tour of combinatorial optimization", John Wiley & Sons Inc (1985).
[15] M. Fang, Layout Optimization for Point-to-Multi-Point Wireless Optical Networks Via Simulated Annealing & Genetic Algorithm", Master Project, University of Bridgeport, Fall, (2000).
[16] R. El-Agmy, H. Bulte, A. Greenaway, et al., Optics Express, **13,** 6085 (2005).
[17] M. T. Vakil-Baghmisheh, A., Navarbaf, "A Modified very Fast Simulated Annealing Algorithm", p. 61, (2008).
[18] C. Paterson, I. Munro, J. Dainty, Optics Express, **6,** 175 (2000).
[19] M.R.N. Avanaki, S. A. Hojjatoleslami, M. Paun, S. Tuohy, A. Meadway, G. Dobre, A. Gh. Podoleanu, Proceedings of Mathematical Methods and Applied Computing, WSEAS, p. 669, (2009).
[20] M.R.N. Avanaki, Y. Long, M.A. Paun, S. A. Hojjatoleslami, A. Gh. Podoleanu, J. Optoelectron. Adv. Mater. **14,** 976 (2012).

*Corresponding author: maria-alexandra.paun@epfl.ch